

Central European Journal of Medicine

Wear debris from hip prostheses characterized by electron imaging

Research Article

Matevž Topolovec¹, Ingrid Milošev^{1,2*}, Andrej Cör^{1,3}, Roy D. Bloebaum^{4,5}

1 Valdoltra Orthopaedic Hospital, Jadranska c. 31, 6280 Ankaran, Slovenia

2 Jožef Stefan Institute, Department of Physical and Organic Chemistry, Jamova 39, 1000 Ljubljana, Slovenia

3 Faculty of Health Science, University of Primorska, Polje 42, 6310 Izola, Slovenia

4 Bone and Joint Research Laboratory, DVA SLC HCS, Salt Lake City, Utah, USA

5 Department of Orthopaedics, University of Utah School of Medicine, Salt Lake City, Utah, USA

Received 7 November 2012; Accepted 6 January 2013

Abstract: The characterization of wear particles is of great importance in understanding the mechanisms of osteolysis. In this unique study, thirty-one tissue samples were retrieved at revision surgeries of hip implants and divided into four groups according to the composition of metal prosthetic components. Tissue samples were first analyzed histologically and then by scanning electron microscopy (SEM) combined with back-scattered electron imaging and energy dispersive X-ray spectroscopy. Therefore, particles were studied directly in situ in tissue sections, without the requirement for particle isolation. The composition of metal wear particles detected in the tissue sections corresponded to the composition of the implant components. A considerable number of large metal particles were actually clusters of submicron particles. The clustering of submicron particles was observed primarily with CoCrMo (cobalt-chromiummolybdenum) and, to a lesser extent, for stainless steel particles. SEM secondary and back-scattered electron imaging was an appropriate and selective method for recognizing the composition of metal particles in the in situ tissue sections, without destroying their spatial relationship within the histology. This method can be used as a screening tool for composition of metal and ceramic particles in tissue sections, or as an additional method for particle identification.

Keywords: Hip prosthesis • Metal wear particles • Histology • Energy dispersive X-ray spectroscopy • Scanning electron microscopy · Back-scattered electron imaging

© Versita Sp. z o.o.

1. Introduction

The long-term clinical performance of joint replacements has largely been determined by the process of aseptic loosening [1]. In this process, the generation of wear debris, especially polyethylene, and their biological effects on periprosthetic tissues are an important factor determining implant removal [1-3]. Implantation of hip prostheses in younger, more active patients has led to a renewed interest and development of third-generation hard-on-hard bearings, including metal-on-metal (MOM) and ceramic-on-ceramic (COC). In these bearings the polyethylene has been avoided which hypothetically should lead to a reduced wear rate and, consequently, a diminished appearance of osteolysis [4,5]. However, osteolysis continues to be encountered in both the thirdgeneration MOM [6] and COC bearings [7].

Although the actual volumetric wear of MOM and COC bearings appears lower than that of metal-onpolyethylene (MOP) bearings [8], the possible long-term effects of exposure to metal particles remains a major concern. Nano-sized particles, ranging from 25 to 50 nm [9] for MOM bearings, could be phagocytosed and/ or pinocytosed more readily than microparticles and cause more mitochondrial and DNA damage [10]. Metal particles have been shown to be more cytotoxic than alumina ceramic wear particles [11].

Lymphoreticular dissemination of metal particles

after primary joint replacements can occur within six months after surgery [12]. Because of the nano-size of the metal particles, the true extent of their dissemination is not yet known. They can potentially have harmful effects on the immune system, the kidney, the nervous system and other organ systems [2]. Furthermore, elevated serum levels of cobalt and chromium in patients with MOM total hip replacements also raised concerns over their potential toxicity [13].

The biological response to metal wear particles depends on their size, shape and chemical composition [1,10-12,14-17]. A precise characterization of the particulate wear debris generated in vivo has become crucial for the understanding of their bioreactivity. Two methods have been used for wear debris evaluation: the isolation and the non-isolation methods. For the former, wear debris has been isolated from periprosthetic tissue. To digest the tissue, alkaline, acid [18,19] and enzyme digestion techniques have been used [20-22]. When using acid or alkaline chemical reagents, however, metal particle size and shape may change [18]. A non-isolation method has been based on a direct evaluation of tissue sections generally using microscopy with transmitted or polarized light [23].

The purpose of our study was to explore the possibility of using scanning electron microscopy (SEM), complemented with secondary and back-scattered electron imaging (BSE) along with energy dispersive X-ray spectroscopy (EDS), for the identification of metal and ceramic particles directly in tissue samples retrieved from aseptically loosened hip prostheses. Periprosthetic tissues of different hip prostheses were analyzed microscopically with particulates *in situ* and correlated with the results of histological analysis.

2. Patients, materials and methods

2.1 Patients and implants

This study had received Institutional Review Board approval. Periprosthetic tissue samples were collected from different sites around the hip prostheses revised for aseptic loosening, including pseudo-capsular tissue, and interfacial acetabular and femoral membranes. According to the type of the implant material, type of implant fixation and the bearing combination, study samples were divided into four groups (below). Patients undergoing revision surgery for septic loosening were not included. Infection was ruled out based on clinical symptoms and the results of laboratory tests (CRP, lymphocyte count, and results of microbiological and histological analyses).

Group I comprised samples retrieved from twelve patients with MOM bearings. The mean patient age at implantation was 58 years (range, 36 to 66 years) and the mean time between the first and revision surgeries (time in situ) was 91 months (range, 29 to 138 months). The initial diagnosis was osteoarthritis for ten patients and avascular femoral head necrosis for two patients. The indications for revision surgery were cup loosening for nine patients, stem loosening for two patients, and both cup and stem loosening for one patient. Patients received cementless acetabular components consisting of a threaded shell made of commercially pure (c.p.) titanium, and an ultrahigh molecular weight polyethylene liner with metal inlay (a so called sandwich-design). Metal inlay and femoral heads were made of Sikomet SM21 low carbon Co-28Cr-6Mo (cobalt-chromiummolybdenum) alloy (Bicon-Plus, Plus Orthopedics, Rotkreuz, Switzerland). The femoral stems were of different designs, but they were all cementless and made of titanium (Ti)-based alloys (Table 1) by different manufacturers (Plus Orthopedics, Rotkreuz, Switzerland; Lima, Udine, Italy; WaldemarLink GmbH&Co. KG, Hamburg, Germany; Allopro AG, Baar, Switzerland).

Group II comprised samples retrieved from five patients with ceramic-on-polyethylene (COP) bearings. The mean patient age at implantation was 45 years (range, 32 to 58 years) and the mean time *in situ* was 191 months (range, 179 to 199 months). The initial diagnosis was primary osteoarthritis for two patients, avascular femoral head necrosis for two patients and posttraumatic osteoarthritis for one patient. The indications for revision surgery were stem loosening for four patients, and cup and stem loosening for one patient. Patients received cementless acetabular components consisting of a threaded shell made of commercially pure (c.p.) titanium, a polyethylene liner (RCM, Cremascoli, Verona, Italy) and an alumina ceramic femoral head. The femoral stems were cementless and made of Ti-based alloys.

Group III included samples retrieved from six patients with cemented metal on polyethylene (MOP) bearings. The mean patient age at implantation was 57 years (range, 49 to 65 years) and the mean time *in situ* was 256 months (range, 131 to 336 months). The initial diagnosis was osteoarthritis for all six patients. The indications for revision surgery were cup and stem loosening for five patients, and stem loosening for one patient. Patients received cemented acetabular polyethylene cups. The femoral stems were a cemented monolithic Charnley-Müller-type made of CoCrMo alloy (Alivium, Zimmer, London, England). For cementation, polymethylmethacrylate (PMMA)-based cement with either BaSO₄ (barium sulfate) or ZrO₂ (zirconium dioxide) as a radiopaque agent was used.

Group IV included samples retrieved from eight patients with cementless MOP bearings. The mean patient age at implantation was 53 years (range, 37 to 60 years) and the mean time *in situ* was 173 months (range, 107 to 253 months). The initial diagnosis was osteoarthritis for all eight patients. The indications for revision surgery were stem loosening for six patients, and cup and stem loosening for two patients. Patients received cementless acetabular cups made of high-density polyethylene (RM Robert Mathys, Bettlach, Switzerland) and stainless steel (AISI 316L, Lima, Udine, Italy) femoral heads. The femoral stems were cementless isoelastic stems made of polyoxymethylene (polyacetal) resin with a central stainless-steel core and two stainless steel screws (RM Robert Mathys, Bettlach, Switzerland).

Table 1. Summary of materials in the implant components of various groups, and metals identified in wear particles in tissue sections by energy dispersion X-ray spectroscopy (EDS).

Group	Material of femoral stem	Material of femoral head	Material of acetabular cup	Elements identified in wear particles by EDS
ı	Ti-6Al-7Nb Ti-6Al-4V	Co-28Cr-6Mo	Ti, polyethylene, Co-28Cr-6Mo	Ti, Al, Co, Cr, Mo
II	Ti-6Al-4V	Al_2O_3	Ti, polethylene	Ti, Al, V
III	Co-28Cr-6Mo	Co-28Cr-6Mo	polyethylene	Co, Cr, Mo, Zr, Ba, S
IV	polyacetal, Fe-18Cr-14Ni- 3Mo	Fe-18Cr-14Ni- 3Mo	polyethylene	Fe, Cr, Ni, Mn, Mo

2.2 Preparation of specimens for analysis

One tissue specimen was analyzed for each patient (giving a total of thirty-one tissue sections). When more tissues samples were available per patient, the highest-quality sample was chosen for analysis (i.e. those without necrosis or bone chips). Specimens were fixed in 10% neutral buffered formalin and embedded in paraffin. Serial 5 µm thick paraffin sections were cut from each block using a microtome. The first section from each block was used for routine histological analysis. The section was stained with hematoxylin and eosin (Richard-Allan Scientific, Kalamazoo, MI, USA) and examined with a light and polarized microscope (Eclipse 80i, Nikon, Japan) equipped with digital camera (DXM1200 F, Nikon, Japan). The degree of metallosis was graded according to the modified Mirra classification [24].

The second section was used for electron microscopy analysis. The section was placed in a warm bath (42°C) and mounted on a glass slide, followed by 2 hours stabilization in an oven at 60°C. The specimens were deparaffinized, placed in a desiccator overnight and carbon coated (using a Cressington 208 Carbon, Cressington Scientific Instruments Ltd., Watford Hertfordshire, UK) for approximately 25 s. A current of 10 mA with a potential of 9 V was used. The vacuum in

the coater was approximately 356 milliTorr. In addition, a glass slide without periprosthetic tissue sections was coated to serve as a control for the EDS analysis.

2.3 Electron microscope analysis

The samples were analyzed with a scanning electron microscope (SEM) (JEOL JSM-6100, Peabody, MA, USA) with a back-scattered electron (BSE) imaging window in conjunction with an energy dispersion X-ray spectrometer and associated analysis software (Noran System Six v2.2, Thermo Fisher Scientific, Madison, WI, USA). The parameters were adjusted as follows: working distance of 15 mm, voltage of 30 kV, analysis counts per second between 1500 and 2500 (dead time approximately 25%) and an aperture setting of 70 μm.

The BSE technique employs the atomic number contrast principle to differentiate metals and ceramics in a sample [16,25]. Due to the nature of the electron microscopy method, it cannot be used to identify polyethylene particles. In BSE images, the metal particles were seen as white spots due to their higher atomic number than that of the non-metallic carbon elements in the soft tissue and resin. The tissue sections were first analyzed in a BSE mode at 500× magnification by manually moving the electron microscope stage in the x- and y-coordinates over the entire sample. Once a metal particle, or cluster of metal particles, was detected, EDS was performed. The particles were then magnified at 2000×, and a BSE image was taken. Remaining at the identical location, a SEM secondary image was also taken. On each tissue section, four different locations were investigated. Twelve images were recorded for each section. The 2048 × 2048 pixel BSE images of metal particles were analyzed by the image analysis software. On each 2000× BSE image, the maximum dimension of each particle and/or cluster bigger than 400 nm was measured. When particles were clustered, we only provided the size of the cluster using calibrated micron bars of the image analysis software. The sizes of the particles and clusters are presented as mean value ± standard deviation (SD), with their range interval.

3. Results

Demographic data of the patients differ among the groups, especially with the time the prostheses were *in situ*. However, the aim of our study was to compare the groups in terms of composition and structure of metal and ceramic particles identified, and not in terms of other parameters.

BSE and secondary SEM images obtained at 2000× magnification and EDS spectra recorded for

various metal particles are presented in Figure 1-4. These figures illustrate the necessity of BSE imaging in identifying and analyzing metal and ceramic particles. Whereas the metal particles could not be differentiated from the rest of the tissue on the secondary SEM images (Figure 1-4, image b), they were clearly distinguished as bright white spots on the BSE images (Figure 1-4, images a). For each group of samples, the materials of the acetabular and femoral components of the implants, and the elements identified in particles present in the tissue resins by EDS, are summarized in Table 1. Metals identified as wear particles in individual samples of each group are presented in Table 2. The elements identified in the glass slide control were carbon, sodium, magnesium, silicon, calcium, iodine, aluminum. Several of these elements are present in the tissues as well, as evident from the EDS spectra given in Figure 1-4.

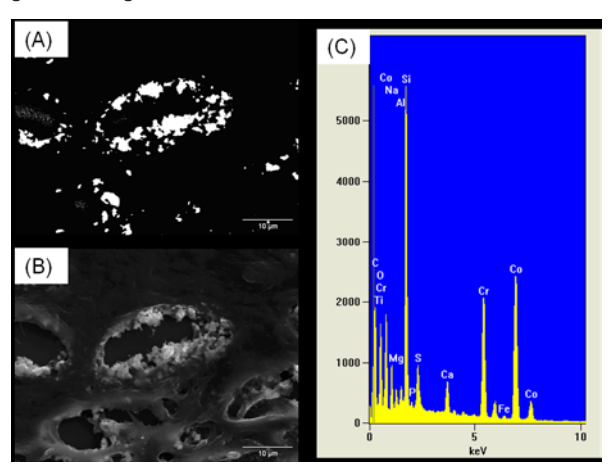


Figure 1. (a) BSE image at 2000× magnification, (b) SEM image at 2000× magnification, and (c) EDS spectrum for CoCrMo particles detected in group I.

In group I, two types of metal particles originating from the prosthesis were identified: CoCrMo and Ti particles (Tables 1, 2). In the majority of cases (nine out of sixteen), both CoCrMo and Ti-based particles were detected. The example of CoCrMo particles can be seen in Figure 1. These particles originate exclusively from the MOM bearing. Titanium-based particles may originate from the Ti cup of the acetabular component, or from the Ti-based femoral stem. The larger amount of Ti particles was usually related to the cases revised for stem loosening. In three out of twelve cases, only Ti particles were detected, without any CoCrMo particles. Two of these cases were revised for stem loosening, which supports the facts that the increased quantity of titanium particles originated from the loosened stem.

When the size of the particles was considered, we distinguished between individual particles and the size

Table 2. Chemical analysis of metal particles by EDS and grade of metal particles by histological analysis for individual samples of the four groups tested. Elements Fe (iron), Cr (chromium), Ni (nickel), Mn (manga-

nese) written in italic are considered to be contamination.

	nese) written in italic are considered to be contamination.					
Sample number	Elements identified in section	Gradation of metal particles in tissue sections by histology				
		Group I				
29	Ti, Al		2+			
101	Ti, Al, Co, Cr,	Fe	2+			
125		Fe, Cr, Ni, Mn	2+			
266		Fe, Cr, Ni, Mn	1+			
292	Ti, Co, Cr	Fe, Mn	2+			
416	Ti, Co, Cr, Mo	Fe, Mn	2+			
422	Ti, Co, Cr, Mo	Fe, Ni	2+			
474	Ti, Al	Fe	1+			
550	Ti, Al, Co, Cr, Mo	Fe, Ni, Mn	2+			
627	Ti, Al		1+			
681	Ti, Al, Co, Cr, Mo	Fe	1+			
721	Ti, Al, Cr	Fe	1+			
		Group II				
39	Ti, Al, V	Fe, Cr, Ni, Mn	2+			
245	Ti, Al, V	Fe, Cr, Mn	2+			
312	Ti, Al, V		1+			
353	Ti, Al, V		1+			
644	Ti, Al, V		1+			
Group III						
78	Zr	Fe	2+			
94	Co, Cr, Mo, Ba, S	minor Fe, Mn	1+			
247	Co, Cr, Mo	Fe , Mn	1+			
345	Co, Cr, Mo, Zr	minor Fe, Mn	1+			
379	Co, Cr, Mo, Ba, S	Fe, Mn	1+			
693	Zr	Fe, Ni, Cr, Mn,	1+			
		Group IV				
424	Fe, Cr, Ni, Mn, Mo		3+			
425	Fe, Cr, Ni, Mn, Mo		1+			
426	Fe, Cr, Ni, Mn, Mo		3+			
433	Fe, Cr, Ni, Mn, Mo		1+			
495	Fe, Cr, Ni, Mn,		2+			
556	Fe, Cr, Ni, Mn		1+			
571	Fe, Cr, Ni, Mn		1+			
716	Fe, Cr, Ni, Mn		1+			

of clusters. Secondary SEM images showed that detected metal particles often appeared in clusters containing submicron-sized particles (Fig. 1). The particles smaller than 400 nm were not measured. Besides submicron particles, particles in the micron range were also present. The clustering of particles was observed primarily for CoCrMo areas. In this group twenty-eight clusters and eighty-two particles were analyzed. The mean size measured on 28 CoCrMo clusters was 2.9 ± 1.8 µm (range, 0.5 to 7.6 µm). On the contrary, Ti particles appeared as individual particles and the clustering effect was not observed. The particles were similar to those observed in group II. Various shapes of the titanium particles were observed: round, oval and elongated. Most Ti particles had an irregular shape. The mean size measured on 82 Ti particles was 2.5 ± 3.6 µm (range, 0.4 to 17.3 µm).

Another type of particle identified in group I, and also in the other three groups, was stainless steel (Fe, Cr, Ni, Mo) (Table 2). In two cases of group I (125 and 266) this was the only type detected. These particles do not originate from the material of implant components and are assumed to be contaminants.

In group II, the diversity of particles was smaller than in group I. The only metal particles detected in all the samples were Ti-based particles (Tables 1, 2). Again, as in group I, the clustering was not observed but, instead, relatively large, individual Ti-based particles were present (Fig. 2). The number of particles analyzed in this group was twenty-six. The mean size measured on 26 Ti particles was $4.3 \pm 2.8 \ \mu m$ (range, $0.8 \ to \ 11.0 \ \mu m$).

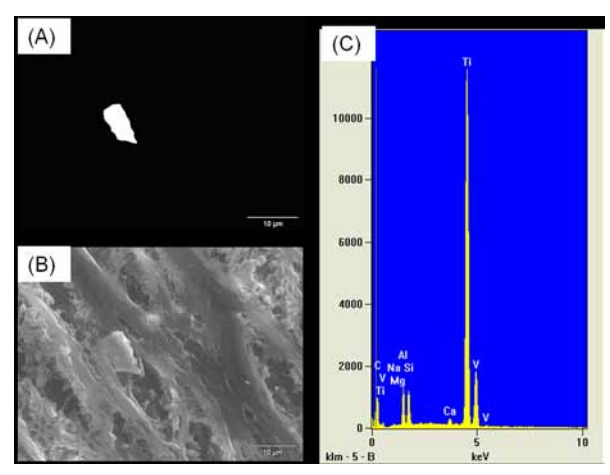


Figure 2. (a) BSE image at 2000× magnification, (b) SEM image at 2000× magnification, and (c) EDS spectrum for Ti particles detected in Group II.

The only metal particles detected in group III were CoCrMo particles, consistent with the composition of the implant material (Tables 1, 2). Similar to group I (Fig. 1), CoCrMo particles were present mainly as clusters of sub-micron particles on secondary SEM imaging, and also as micron-sized particles. Eleven clusters were analyzed in this group. The mean size measured on 11 CoCrMo clusters was 3.2 \pm 1.0 μm (range, 1.9 to 5.4 μm). In four cases, BaSO $_{\!_4}$ or Zr-containing particles were detected (Fig. 3). These particles are added as radio-opaque agents to PMMA bone cement. Whereas PMMA was dissolved by chemicals during the preparation of tissue resin for histological analysis, BaSO $_{\!_4}$ and ZrO $_{\!_2}$ are resistant to this procedure and remained in the resin.

The metal wear particles in group IV were identified as stainless steel (Tables 1, 2). Similar to CoCrMo particles, a clustering effect was observed for stainless steel particles, although to a lesser extent (Fig. 4), so it was possible to measure individual particles. Thirty-five particles were analyzed in this group. The mean size mea-

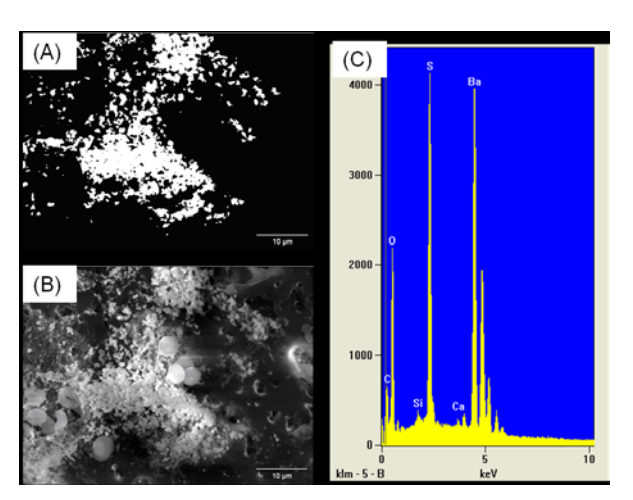


Figure 3. (a) BSE image at 2000× magnification, (b) SEM image at 2000× magnification, and (c) EDS spectrum for BaSO₄ particles detected in group III.

sured on 35 stainless steel particles was $4.7 \pm 2.9 \, \mu m$ (range, 1.9 to $13.7 \, \mu m$). In this group, the entire implant was made of stainless steel. It is thus reasonable to assume that the majority of these particles originate from a wear process, although a small proportion of these may be contaminants, as observed in other groups (Table 2). It was not possible to differentiate the origin of these particles based on their morphology, i.e. whether they originate from the wear of implant components or from contamination.

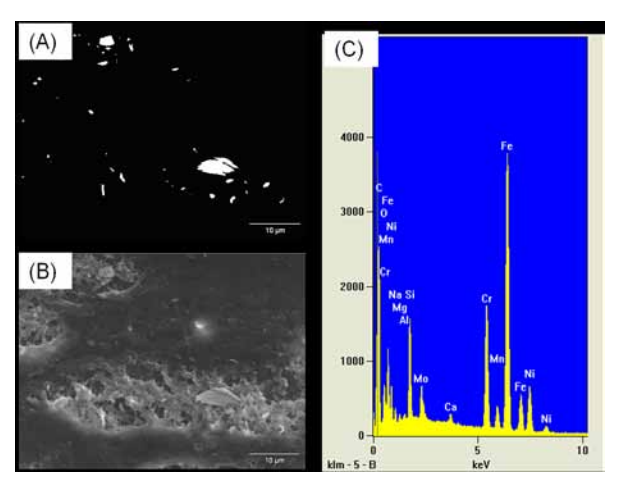


Figure 4. (a) BSE images at 2000× magnification, (b) SEM image at magnification 2000×, and (c) EDS spectrum for stainless steel particles detected in group IV.

Overall, 143 particles and 39 clusters were analyzed in four groups of samples.

Examples of histological tissue sections graded from 1+ to 3+ are presented in Fig. 5a-d. The gradation of metal particles for individual samples in each group tested is given in Table 2, along with the composition of metal wear particles obtained by secondary SEM/

BSE/EDS analysis. Metal particles were detected in all samples. This correlates well with the results obtained by histological examination. The gradation of metal particles in the tissue ranged from 1+ (metal wear debris is seen as greyish blue colored histiocyte cytoplasm) to 3+ (metal wear debris with innumerable metal particles that obscure the morphology of cells and tissue). The percentages of cases with differing amounts of metal wear debris in periprosthetic tissue samples are given in Fig. 6. Only in group I was the percentage of samples graded 2+ (metal wear debris within dusty black histiocytes) higher than the percentage of samples graded 1+. In all other groups, the percentage of samples graded 1+ predominated. Group IV contained two samples graded 3+ but, compared to group I, the percentage of grade 1+ was higher. Therefore, based on the histological results, it can be concluded that in Group I, the percentage of samples with a higher proportion of metal particles (graded 2+) was greater than in the other three groups. No clear correlation could be established between reason for revision, i.e. cup or stem loosening, or both, and the gradation of metal particles.

4. Discussion

Wear particles are considered to be the major contributors to the development of aseptic loosening [1]. The mechanism of cell damage appears to be different after exposure to wear particles of different sizes,

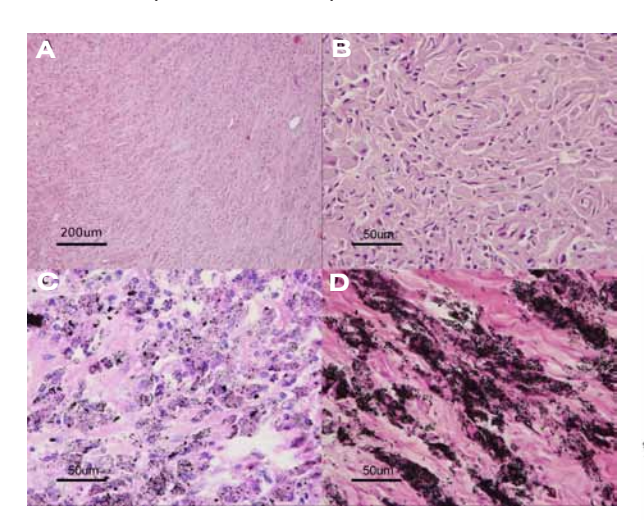


Figure 5. Microscopic pictures (a-d) of periprosthetic tissue around metal-on-metal hip prostheses.

(a) Macrophages and giant cells are the major characteristic of granulomatous tissue with different amount of metal particles; (b) 1 + metal wear debris is seen as greyish blue colored histiocyte cytoplasm; (c) 2+ metal wear debris within dusty black histiocytes; (d) 3+ metal wear debris with innumerable metal particles that obscure the morphology of cells and tissue.

composition and morphology [10,26]. The reactivity of wear debris in tissue cultures depends on the relative proportion or concentration of metal in the wear debris [27]. It is therefore important to investigate the structure and properties of wear particles in detail. In the present study we analyzed metal wear debris by a non-destructive method, directly in periprosthetic tissue resins by secondary SEM combined with BSE and EDS. The composition of metal wear particles detected in the tissue sections corresponded to the constituents of the implant components for histological comparison. This method is therefore suitable for analyzing the composition of metal wear particles in situ, which is its main advantage. Although in this particular study we have not compared this non-isolation method with any isolation methods which use digestion, it has been reported that different types of digestion protocols may change metal particle size and shape may change [18].

Wear particles can be generated by both articulating and non-articulating surfaces of metallic components of the prostheses, such as the femoral heads, acetabular cup backings and loose femoral stems [28]. Results of the present study confirm these observations. In group I it was possible to differentiate particles originating from the articulating, weight-bearing surface (CoCrMo particles) and particles generated by non-articulating surfaces (Ti-based particles). The majority of CoCrMo particles from the bearing surface were submicron particles which tend to agglomerate into micron-size clusters. When the size of the particles was considered, we therefore differentiated between the size of individual particles and the size of clusters of particles. The clustering of particles was noted primarily for CoCrMo particles in group I (Fig. 1) and, to a considerably lesser extent, for stainless steel particles in group IV (Fig. 4). The size of isolated individual particles from MOM bearings has been shown to be smaller than 100 nm [22,29].

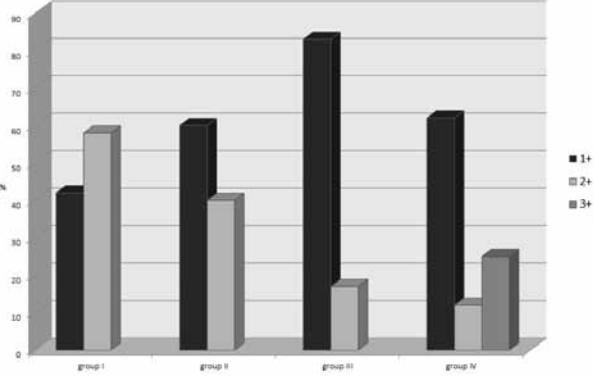


Figure 6. The percentage of cases with different amount of metal wear debris in periprosthetic tissue samples around four groups of prostheses.

The size of the clusters observed correlates with previous reports [21,30]. Spherical CoCr-based particles, sized from sub-micron to 4 μ m, were identified in tissue resins by TEM analysis [30]. Cluster formation of metal particles was also reported by Doorn et al. [21]. Particles isolated by lubricant digestion formed clumps in larger amount than particles isolated from distilled water [29]. The agglomeration of metal particles was also ascribed to an optical effect from multiple layers of small particles packed inside histiocytes [31].

Converse to CoCrMo particles, the formation of clusters was not observed for titanium particles originating from non-articulating surfaces. Instead, they were presented as micron-sized flakes or globule-shaped particles (Fig. 2). These particles originate from wear of the femoral stem since their number is higher in the tissues originating from loose Ti-based femoral stems. These particles may also originate from the acetabular cup backing made of pure Ti (Table 2). According to Maloney et al., the generation of metal stem wear debris may be related to improper implant stability, implant material and the presence of porous coating [32]. The release of Ti particles may be reflected as a systemic effect, as it was reported that patients with loose Ti stem can have an elevated serum titanium concentration [33]. The size of Ti particles we found correlates well with other reports in the literature [21,30]. Spherical or rod-like titanium-based particles ranging from sub-micron to 9 µm were detected by TEM in tissue resins of periprosthetic tissue [30]. Ti-based particles originating from the femoral stem, ranging from 200 to 400 µm in size and from 10 to 20 µm in width, were isolated from periprosthetic tissue by an alkaline digestion method [26].

Besides particles originating from the implant material, we have found other particles from alternative sources. In the group with cemented components, ${\rm BaSO_4}$ and ${\rm ZrO_2}$ granules were detected. Furthermore, in groups II, III and IV we have detected particles of stainless steel which have no clear relationship to the implanted material and probably originate from the contamination induced by surgical instruments at the revision operation and/or microtome blade used for cutting of tissue sections.

We used 5 µm thick tissue sections, which was an optimal thickness for microscopic analysis of histological samples containing wear debris. The thickness was set arbitrarily: narrower sections, especially ones that showed metallosis, were prone to tearing, whilst thicker sections showed lower separability between tissue and metal particles when analysed by back-scattered SEM analysis. In that latter case, edges of the particles located at the deeper levels of tissue resin could not be well distinguished as for the particles located at the surface of the resin. The thickness thus represents a major limi-

tation on determining the precise size and shape of particles, especially particles smaller than 400 nm. These particles could be analyzed using higher magnification; however, we selected the magnification of 2000× as an optimum compromise between time consumption and particle detection. This method may be time-consuming when using higher magnifications. On the other hand, isolation methods such as hydroxide or enzyme digestion require even more time to complete the sample preparation and the analysis.

The purpose of the present study was to check the availability of the method for *in situ* detection of particles and was thus applied to heterogeneous study groups. The method would also be appropriate to study tissue samples taken from different periprosthetic sites within one study group.

Considering the results of histological analysis, it seems that the metal particles are present in higher amounts (higher percentage of grade 2+) in the group I than in other groups. At this stage of our investigation, we are not able to draw any further conclusion based on this result. Namely, the demographic patient data and the time *in situ* in the groups tested were different and created solely on the type of implant material. In order to prove the hypothesis that the tissue samples originating from one group contain metal particles in amount that is significantly higher than in another group, the study would need to be performed in groups that are comparable in terms of demographic patient data, reason for prosthesis revision, and duration that the prosthesis was *in situ*.

5. Conclusions

The presence of metal particles was confirmed by SEM, optical microscopic and histological analyses. Each of these methods is specific: microscopy enables the identification of the composition and size of metal particles; histological analysis was used to grade the quantity of metal particles in situ in tissue. The SEM/BSE/EDS method represents a correlated simple, quick and highly specific way to identify the metal particles in periprosthetic tissue from failed metal implants. The composition of the metal particles and clusters detected correlated with the material of the implant components. The advantage of this method is that it can be applied directly to tissue samples without altering the particle size, morphology and composition, thus offering the opportunity to examine the released particles in situ. The method can be used as a screening tool for identifying the composition of metal particles in various tissue sections, or as an additional method for particle identification. On the other hand, this study has several limitations: the measured size of the particles may be limited by the thickness of tissue sections, and the use of higher magnification is required for the analysis of particles smaller than 400 nm.

References

- [1] Revell PA. The combined role of wear particles, macrophages and lymphocytes in the loosening of total joint prostheses. J. R. Soc. Interface, 2008, 5, 1263-1278
- [2] Keegan GM, Learmonth ID, Case CP. Orthopaedic metals and their potential toxicity in the arthroplasty patient: A review of current knowledge and future strategies. J. Bone Joint Surg. Br., 2007, 89, 567-573
- [3] Willert HG, Bertram H, Buchhorn GH. Osteolysis in alloarthroplasty of the hip. The role of ultra-high molecular weight polyethylene wear particles. Clin. Orthop. Relat. Res., 1990, 258, 95-107
- [4] Essner A, Sutton K, Wang A. Hip simulator wear comparison of metal-on-metal, ceramic-on-ceramic and crosslinked UHMWPE bearings. Wear, 2005, 259, 992-995
- [5] Slonaker M, Goswami T. Review of wear mechanisms in hip implants: Paper II ceramics IG004712. Materials & Design, 2004, 25, 395-405
- [6] Milosev I, Trebse R, Kovac S, Cör A, Pisot V. Survivorship and retrieval analysis of Sikomet metalon-metal total hip replacements at a mean of seven years. J. Bone Joint Surg. Am., 2006, 88, 1173-1182
- [7] Yoon TR, Rowe SM, Jung ST, Seon KJ, Maloney WJ. Osteolysis in association with a total hip arthroplasty with ceramic bearing surfaces. J. Bone Joint Surg. Am., 1998, 80-A, 1459-1467
- [8] Jin Z, Fisher J. Tribology in joint replacement. In: Revel PA (Ed.), Joint replacement technology. Cambridge, Woodhead Publishing Ltd, 2008, 31-55
- [9] Firkins P J, Tipper JL, Saadatzadeh MR, Ingham E, Stone MH, Farrar R, Fisher J. Quantitative analysis of wear and wear debris from metal-on-metal hip prostheses tested in a physiological hip joint simulator. Biomed. Mater. Eng., 2001, 11, 143-157
- [10] Papageorgiou I, Brown C, Schins R, Newson R, Davis S, Fisher J, Ingham E, Case CP. The ef-

Acknowledgments

This study was funded by the Slovenian Research Agency through grant No. J3-0052 and through grant No. BI-US/08-10-019 allowing bilateral collaboration between Slovenia and USA. This material was also based upon work supported in part by the Office of Research and Development (Rehabilitation R&D Service), Department of Veterans Affairs SLC HSC, the Albert and Margaret Hofmann Chair in Orthopaedic Surgery, and the Department of Orthopaedics, University of Utah School of Medicine, Salt Lake City, UT, USA.

- fect of nano- and micron-sized particles of cobalt-chromium alloy on human fibroblasts in vitro. Biomaterials, 2007, 28, 2946-2958
- [11] Germain MA, Hatton A, Williams S, Matthews JB, Stone MH, Fisher J, Ingham E. Comparison of the cytotoxicity of clinically relevant cobalt-chromium and alumina ceramic wear particles in vitro. Biomaterials, 2003, 24, 469-479
- [12] Shea KG, Lundeen GA, Bloebaum RD, Bachus KN, Zou L. Lymphoreticular dissemination of metal particles after primary joint replacements. Clin. Orthop. Relat. Res., 1997, 338, 219-326
- [13] Milosev I, Pisot V, Campbell P. Serum levels of cobalt and chromium in patients with Sikomet metal-metal total hip replacements. J. Orthop. Res., 2005, 23, 526-535
- [14] Catelas I, Campbell PA, Bobyn JD, Medley JB, Huk OL. Wear particles from metal-on-metal total hip replacements: effects of implant design and implantation time. Proc. Inst. Mech. Eng. H, 2006, 220, 195-208
- [15] Goodman SB. Wear particles, periprosthetic osteolysis and the immune system. Biomaterials, 2007, 28, 5044-5048
- [16] RobinsonVNE. Materials characterization using the backscattered electron signal in scanning electron microscopy. Scanning Microscopy, 1987, 1, 107-117
- [17] Sabokbar A, Pandey R, Athanasou NA. The effect of particle size and electrical charge on macrophage-osteoclast differentiation and bone resorption. J. Mater. Sci. Mater. Med., 2003, 14, 731-738.
- [18] Catelas I, Bobyn JD, Medley JB, Krygier JJ, Zukor DJ, Petit A, Huk OL. Effects of digestion protocols on the isolation and characterization of metalmetal wear particles. I. Analysis of particle size and shape. J. Biomed. Mater. Res., 2001, 55, 320-329

- [19] Margevicius KJ, Bauer TW, McMahon JT, Brown SA, Merritt K. Isolation and characterization of debris in membranes around total joint prostheses. J. Bone Joint Surg. Am., 1994, 76, 1664-1675
- [20] Catelas I, Medley JB, Campbell PA, Huk OL, Bobyn JD. Comparison of in vitro with in vivo characteristics of wear particles from metal-metal hip implants. J. Biomed. Mater. Res. B. Appl. Biomater., 2004, 70, 167-178
- [21] Doorn PF, Campbell PA, Worrall J, Benya PD, McKellop HA, Amstutz HC. Metal wear particle characterization from metal on metal total hip replacements: transmission electron microscopy study of periprosthetic tissues and isolated particles. J. Biomed. Mater. Res., 1998, 42, 103-111
- [22] Milosev I, Remskar M. In vivo production of nanosized metal wear debris formed by tribochemical reaction as confirmed by high-resolution TEM and XPS analyses. J. Biomed. Mater. Res. A, 2009, 91, 1100-1110
- [23] Lerouge S, Huk O, Yahia LH, Sedel L. Characterization of in vivo wear debris from ceramic-ceramic total hip arthroplasties. J. Biomed. Mater. Res., 1996, 32, 627-633
- [24] Doorn PF, Mirra JM, Campbell PA, Amstutz HC. Tissue reaction to metal on metal total hip prostheses. Clin. Orthop. Relat. Res., 1996, 329S, 187-205
- [25] Bloebaum RD, Bachus KD, Boyce TM. Backscattered electron imaging: the role in calcified tissue and implant analysis. J. Biomater. Appl., 1990, 5, 56-85
- [26] Shanbhag AS, Jacobs JJ, Glant TT, Gilbert JL, Black J, Galante JO. Composition and morphology of wear debris in failed uncemented total hip re-

- placement. J. Bone Joint Surg. Br., 1994, 76, 60-67
- [27] Daley B, Doherty AT, Fairman B, Case CP. Wear debris from hip or knee replacements causes chromosomal damage in human cells in tissue culture. J. Bone Joint Surg. Br., 2004, 86, 598-606
- [28] Stachowiak GW, Stachowiak GB, Campbell P. Application of numerical descriptors to the characterization of wear particles obtained from joint replacements. Proc. Inst. Mech. Eng. H, 1997, 211, 1-10
- [29] Tipper JL, Firkins PJ, Besong AA, Barbour PSM, Nevelos J, Stone MH, Ingham E, Fisher J. Characterisation of wear debris from UHMWPE on zirconia ceramic, metal-on-metal and alumina ceramic-on-ceramic hip prostheses generated in a physiological anatomical hip joint simulator. Wear, 2001, 250, 120-128
- [30] Shahgaldi BF, Heatley FW, Dewar A, Corrin B. In vivo corrosion of cobalt-chromium and titanium wear particles. J. Bone Joint Surg. Br., 1995, 77, 962-966
- [31] Walker PS, Gold BL. The tribology (friction, lubrication and wear) of all-metal artificial hip joints. Clin. Orthop. Relat. Res., 1996, 329 Suppl, 4-10
- [32] Maloney WJ, Smith RL, Schmalzried TP, Chiba J, Huene D, Rubash H. Isolation and characterization of wear particles generated in patients who have had failure of a hip arthroplasty without cement. J. Bone Joint Surg. Am., 1995, 77, 1301-1310
- [33] Jacobs JJ, Skipor AK, Black J, Urban R, Galante JO. Release and excretion of metal in patients who have a total hip-replacement component made of titanium-base alloy. J. Bone Joint Surg. Am., 1991, 73, 1475-1486